

# Technetium-99m-Labeled HL91 to Identify Tumor Hypoxia: Correlation with Fluorine-18-FDG

Gary J.R. Cook, Stephen Houston, Sally F. Barrington and Ignac Fogelman

Clinical PET Center and Department of Oncology, Guys and St. Thomas' Hospitals, United Medical and Dental Schools, London, United Kingdom

Technetium-99m HL91 is a potential agent for imaging hypoxic tissue in vivo. A pilot evaluation using a prototype formulation assessed efficacy in tumor imaging and compared results with  $^{18}\text{F}$ -fluorodeoxyglucose (FDG) PET. **Methods:** Ten patients with malignant tumors were included. Tumors included carcinoma of the bronchus ( $n = 3$ ), carcinoma of the thyroid ( $n = 2$ ), lymphoma ( $n = 2$ ), soft tissue sarcoma ( $n = 1$ ), carcinoid ( $n = 1$ ) and carcinoma of the breast ( $n = 1$ ). Whole-body planar scans and localized SPECT scans were performed at 1 and 4 hr postinjection of 600 MBq  $^{99\text{m}}\text{Tc}$  HL91. Half-body and localized emission/transmission  $^{18}\text{F}$ -FDG PET scans were performed 60 min postinjection 370 MBq  $^{18}\text{F}$ -FDG in eight patients. Lesion-to-normal tissue background ratios were measured for all  $^{99\text{m}}\text{Tc}$  HL91 and  $^{18}\text{F}$ -FDG PET scans and percentage uptake and standardized uptake values measured for  $^{99\text{m}}\text{Tc}$  HL91 and  $^{18}\text{F}$ -FDG PET, respectively. **Results:** Technetium-99m HL91 showed visible uptake into the tumor area in all seven studies where the tumor was clearly identified by  $^{18}\text{F}$ -FDG PET;  $^{99\text{m}}\text{Tc}$  HL91 uptake was not detected in one study (carcinoid) in which  $^{18}\text{F}$ -FDG was weakly positive. Two further tumors, in which PET correlation was not available, showed accumulation of  $^{99\text{m}}\text{Tc}$  HL91. In two  $^{99\text{m}}\text{Tc}$  HL91 studies, abnormality was apparent only on SPECT images. Lesion-to-normal tissue background ratios for  $^{99\text{m}}\text{Tc}$  HL91 ranged from 1.22/2.53 at 1 hr and 1.33/2.89 at 4 hr on planar images and 1.23/5.2 and 1.67/14.6 on SPECT images, respectively. **Conclusion:** In this study, the use of  $^{99\text{m}}\text{Tc}$  HL91 resulted in uptake in the majority of malignant tumors identified by  $^{18}\text{F}$ -FDG-PET. Technetium-99m HL91 exhibits good imaging characteristics, with imaging at 4 hr providing good lesion-to-normal tissue background ratios, that are further enhanced by SPECT.

**Key Words:** technetium-99m; HL91;  $^{18}\text{F}$ -fluorodeoxyglucose PET; tumor hypoxia

J Nucl Med 1998; 39:99-103

Many malignant tumors are characterized by perfusion heterogeneity, which results in tumor regions that are acutely or chronically hypoxic (1,2). This is clinically important as tumor hypoxia may increase resistance to radiation therapy and to some forms of chemotherapy (3). The recognition of a hypoxic tumor fraction can have implications for therapy. Radiosensitization drug therapy or the use of hyperbaric oxygen are the methods of improving outcome that have been investigated (4,5). It is not possible to predict tumor hypoxia because of both inter- and intratumoral heterogeneity in oxygen status (2,3,6).

Several direct and indirect methods for measuring hypoxia exist (7), but many are invasive or not suitable for routine clinical use. There has, therefore, been much interest in noninvasive methods such as magnetic resonance spectroscopy (8) and imaging of radiolabeled compounds that are selectively retained in regions of hypoxia (9-11).

The PET tracer  $^{18}\text{F}$  misonidazole has been evaluated in several tumors (10) and in the study of ischemic myocardium

(12), but the ready availability of gamma camera imaging has led to the introduction of several single-photon radiopharmaceuticals (9,11,13).

Nitroimidazole-containing compounds have received the most attention. The nitro group undergoes one electron reduction in viable cells to produce a radical anion. In normoxic cells, this intermediate is rapidly reoxidised and can subsequently diffuse out of the cell. In hypoxic tissue, it is further reduced to species that can react with cell components and be retained within the cell. Technetium-99m-labeled ligands containing 2-nitroimidazole show hypoxia selectivity (14), but a complex of core ligands without the nitroimidazole group has shown even greater hypoxia selectivity (11). We have performed a pilot evaluation using such a compound ( $^{99\text{m}}\text{Tc}$  HL91) (Fig. 1) to assess imaging characteristics and efficacy in tumor detection. We have correlated results with  $^{18}\text{F}$ -FDG PET as a gold standard scintigraphic method of tumor localization.

## MATERIALS AND METHODS

**Preparation of  $^{99\text{m}}\text{Tc}$  HL91:**  $^{99\text{m}}\text{Tc}$  HL91 was prepared by reconstitution of a sterile lyophilized kit formulation. Vials were reconstituted with sterile sodium pertechnetate solution to a final radioactive concentration of 200 MBq/ml. The radiochemical purity of each preparation of  $^{99\text{m}}\text{Tc}$  HL91 was determined before use and was found to be greater than 98% on each occasion.

## Patients

Ten patients (seven men, three women; mean age 67 yr) with malignant tumors were included in the study. Tumor types included carcinoma of the bronchus ( $n = 3$ , two squamous cell and one adenocarcinoma), follicular carcinoma of the thyroid ( $n = 2$ ), lymphoma ( $n = 2$ ), soft tissue sarcoma ( $n = 1$ ), carcinoma of the breast ( $n = 1$ ) and malignant carcinoid ( $n = 1$ ). Eight patients had  $^{18}\text{F}$ -FDG-PET performed. Three patients were known to have metastatic tumor sites.

## Imaging

After intravenous injection of 600 MBq  $^{99\text{m}}\text{Tc}$  HL91, whole-body planar scans were performed at 1 and 4 hr using a twin-headed gamma camera in scanning mode (10 min/m) fitted with high-resolution collimators. Localized SPECT acquisitions were made of known tumor regions at 1 and 4 hr with a  $64 \times 30$  sec acquisition over  $360^\circ$  with high-resolution collimation. Images were reconstructed using a Hanning 0.8 filter and presented as transaxial, coronal and sagittal slices.

Using a PET scanner, whole-body scans were performed 1 hr postinjection with 370 MBq  $^{18}\text{F}$ -FDG. Localized, attenuation-corrected scans were acquired over the tumor region.

## Image Analysis

Three-dimensional reconstructed projection PET images were nominally denoted as "planar" PET images. Regions of interest (ROIs) were drawn around the tumor on planar and tomographic  $^{99\text{m}}\text{Tc}$  HL91 and  $^{18}\text{F}$ -FDG images. For tomographic slices, counts were averaged for all of the slices in which tumor activity was

Received Dec. 12, 1996; revision accepted Mar. 25, 1997.

For correspondence or reprints contact: Dr. G.J.R. Cook, Department of Nuclear Medicine, Guys Hospital, London SE1 9RT, UK.

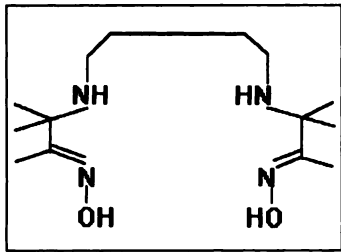


FIGURE 1. Chemical structure of HL91.

visible. Normal tissue background regions (N) were taken from qualitatively normal regions on the opposite side of the body and background activity (B) from a region outside of the body contour. All tumor (T) and normal tissue data were background-corrected before calculation of lesion-to-normal tissue ratios for planar and tomographic images. Absolute uptake of  $^{99m}\text{Tc}$  HL91 was measured from planar-decay corrected and background and normal-tissue background-subtracted tumor regions and expressed as a percentage of injected dose. Decay corrected whole-body counts at 1 hr were taken to represent 100% of injected activity. Standardized uptake values (SUVs) were calculated from  $\text{SUV} = \{(\text{activity in ROI}/\text{vol. of ROI})/(\text{injected activity}/\text{weight of patient})\}$  and were corrected for partial volume effects.

**RESULTS**

At 1 hr postinjection,  $^{99m}\text{Tc}$  HL91, the distribution of activity includes skeletal muscle with minimal blood-pool activity. There is evidence of both hepatic and, to a lesser extent, renal clearance, resulting in small bowel and bladder activity. At 4 hr,

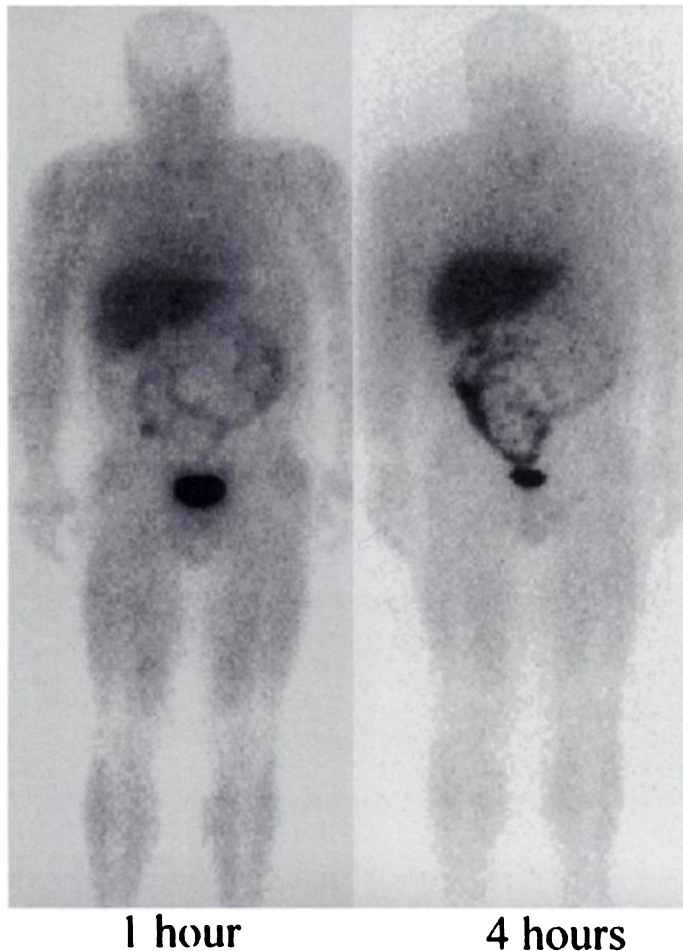


FIGURE 2. Normal distribution of  $^{99m}\text{Tc}$  HL91 at 1 and 4 hr.

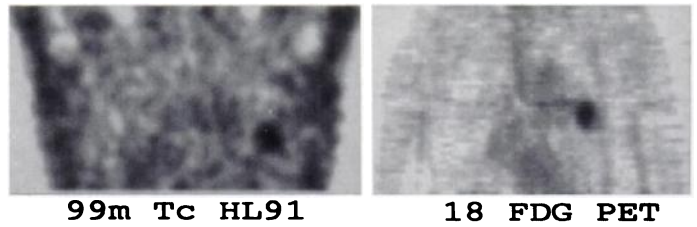


FIGURE 3. Coronal 4-hr  $^{99m}\text{Tc}$  HL91 SPECT (left) and  $^{18}\text{F}$ -FDG PET (right) images of a squamous cell carcinoma of the bronchus.

there is significant clearance of activity from skeletal muscle with continued hepatobiliary and renal excretion into small and large bowel and bladder (Fig. 2).

After injection of  $^{99m}\text{Tc}$  HL91, tumor activity was identified in five patients on planar images corresponding to regions identified by  $^{18}\text{F}$ -FDG PET and all five were similarly identified by SPECT (Fig. 3). A similarity in the spatial distribution of activity between  $^{99m}\text{Tc}$  HL91 and  $^{18}\text{F}$ -FDG was noted (Fig. 4). For two other patients, tumor localization after injection of  $^{99m}\text{Tc}$  HL91 was only possible by SPECT imaging. One patient (carcinoid) did not show uptake into known tumor deposits identified on  $^{18}\text{F}$ -FDG PET. The remaining two patients did not have  $^{18}\text{F}$ -FDG PET scans performed, but tumor activity was identified after  $^{99m}\text{Tc}$  HL91 injection in a histologically confirmed squamous cell carcinoma of the bronchus and carcinoma of the breast (Table 1).

Three patients had more than one tumor region identified with  $^{18}\text{F}$ -FDG PET. In one of these patients, with carcinoid lesions, none of the lesions were detected after injection of  $^{99m}\text{Tc}$  HL91. For the remaining two patients, the majority of the tumor regions also were identified by planar or SPECT imaging of  $^{99m}\text{Tc}$  HL91. One patient with follicular carcinoma of the thyroid showed uptake of  $^{99m}\text{Tc}$  HL91 into tumor metastasis to the base of skull but not to two further, but smaller, bone metastases identified by  $^{18}\text{F}$ -FDG PET. Uptake of  $^{99m}\text{Tc}$  HL91 also was seen in the third patient with multiple  $^{18}\text{F}$ -FDG PET lesions at both metastatic sites in the neck from follicular carcinoma of the thyroid.

In six out of seven patients, where tumor activity was identifiable on planar  $^{99m}\text{Tc}$  HL91 images, an increase in absolute uptake was measured. One patient showed an apparent fall in absolute uptake over time. This is likely to be artifactual as it only occurred on planar and not on SPECT imaging. This patient with lymphoma of the skull had an infected, inflammatory mass overlying the tumor. Nonspecific activity, due to the increased vascularity of the overlying lesion, could not be separated on planar images at 1 hr and gave a falsely high measured activity within the lesion and could be separated by

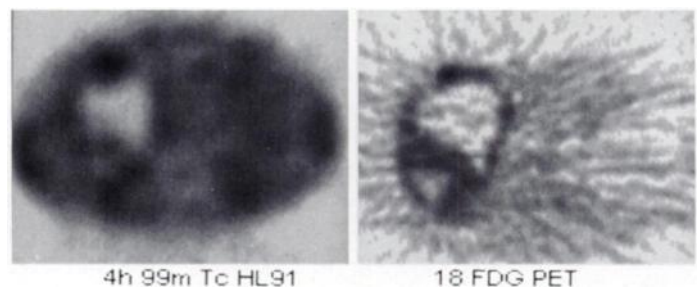


FIGURE 4. Technetium-99m HL91 SPECT (left) and  $^{18}\text{F}$ -FDG PET (right) transaxial slices through the thorax of a patient with a large right-sided soft tissue sarcoma. Nonviable necrotic tissue lies in the center of the tumor. There is accumulation of  $^{18}\text{F}$ -FDG in the periphery of the tumor in a pattern that is similar to the  $^{99m}\text{Tc}$  HL91 study.

**TABLE 1**  
Details of <sup>99m</sup>Tc HL91 and <sup>18</sup>F-FDG Scan Results

Subject	Tumor	Planar HL91	SPECT HL91	PET FDG	Change in absolute activity between 1 and 4 hr
1	Bronchus (squamous cell carcinoma)	+	+	+	↑
2	Bronchus (squamous cell carcinoma)	+	+	Not performed	↑
3	Bronchus (adenocarcinoma)	+	+	+	↑
4	Thyroid (follicular carcinoma)				
i	L neck metastasis	+	+	+	↑
ii	R neck metastasis	+	+	+	↑
5	Thyroid (follicular carcinoma)				
i	Base of skull metastasis	-	+	+	Not visible on planar
ii	Vertebral metastasis	-	Not performed	+	Not visible on planar
iii	Femoral metastasis	-	Not performed	+	Not visible on planar
6	Carcinoid				
i	Supraclavicular lymph node	-	-	Weak +	Not visible on planar
ii	Liver metastases	-	Not performed	Weak +	Not visible on planar
7	Breast carcinoma	+	+	Not performed	↑
8	Tonsillar lymphoma	-	+	+	Not visible on planar
9	Skull lymphoma	+	+	+	↓
10	Sarcoma of the lung	+	+	+	↑

+ = Tumor activity present.  
- = Tumor activity not identified.  
↑ and ↓ = Increase and decrease in measured absolute activity in <sup>99m</sup>Tc HL91 planar studies between 1 and 4 hr, respectively.

SPECT. At 4 hr, there was almost complete clearance from the inflammatory mass, as seen by SPECT, leaving only tumor-specific activity (Fig. 5).

Tumor-to-normal tissue background ratios (T:N) for planar and tomographic <sup>99m</sup>Tc HL91 and <sup>18</sup>F-FDG PET are listed in Table 2. For <sup>99m</sup>Tc HL91 planar images, the mean T:N values increased from 1.65 to 1.76 at 1 and 4 hr postinjection, respectively (Fig. 6).

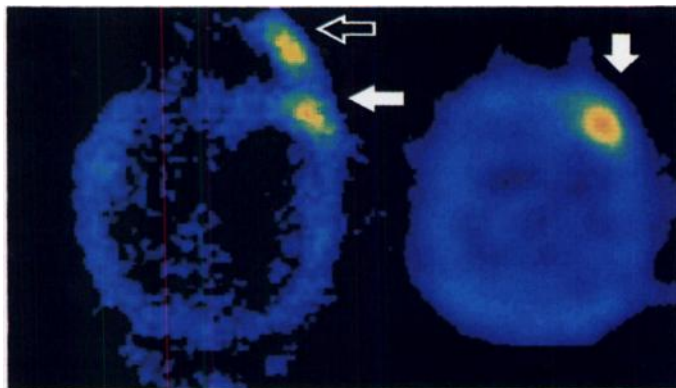


**FIGURE 5.** One hour (left) and 4 hr (right) transaxial SPECT slices through the skull in a patient with lymphoma of the skull. Nonspecific activity in an overlying inflammatory mass reduces with time (open arrow) leaving specific tumor activity (arrows).

SPECT imaging showed consistently higher T:N values than planar imaging (range 1.23 to 14.6). For two patients, the tumor site that was not visible on planar images was clearly identified by SPECT. In all cases, planar and tomographic <sup>18</sup>F-FDG PET imaging resulted in higher T:N ratios than those obtained from <sup>99m</sup>Tc HL91 imaging.

## DISCUSSION

In this study, <sup>99m</sup>Tc HL91 has shown specific localization in the majority of malignant tumors identified by <sup>18</sup>F-FDG PET. Tumor-to-normal tissue background activity ratios are sufficient for tumors to be readily identified by SPECT imaging and in most cases also by planar imaging. Tumor activity is more easily identified at 4 hr rather than at 1 hr postinjection mainly due to a reduction in background activity.

The identification of tumor hypoxia is currently an area of intense interest because tumor hypoxia may increase resistance to radiotherapy and some forms of chemotherapy. Once tumor hypoxia is identified, more aggressive treatment regimens may be selected to reduce hypoxic resistance. Although many methods of measuring tumor hypoxia have been described, an accurate, noninvasive, imaging method would be preferable for patients in the clinical setting.

Fluorine-18-fluoromisonidazole is probably the most studied tracer for imaging hypoxia and has been used in tumors and ischemic myocardium (10,12). A radiopharmaceutical labeled

**TABLE 2**  
Tumor-to-Normal Tissue Background Ratios for <sup>99m</sup>Tc HL91 at 1 and 4 Hours and for <sup>18</sup>F-FDG PET

	HL91 planar*	HL91 SPECT*	FDG planar	FDG tomography	HL91% uptake	FDG SUV
1 hr	1.22–2.53 (1.65) <sup>†</sup>	1.23–5.2 (2.05)	1.51–3.37 (2.6)	1.37–12.8 (6.45)	0–0.04%	0.85–8.8 (5.64)
4 hr	1.33–2.89 (1.76)	1.67–14.6 (3.65)			0–0.07%	

\*Patient with carcinoid tumor with no apparent uptake omitted.

<sup>†</sup>Mean values in parentheses.

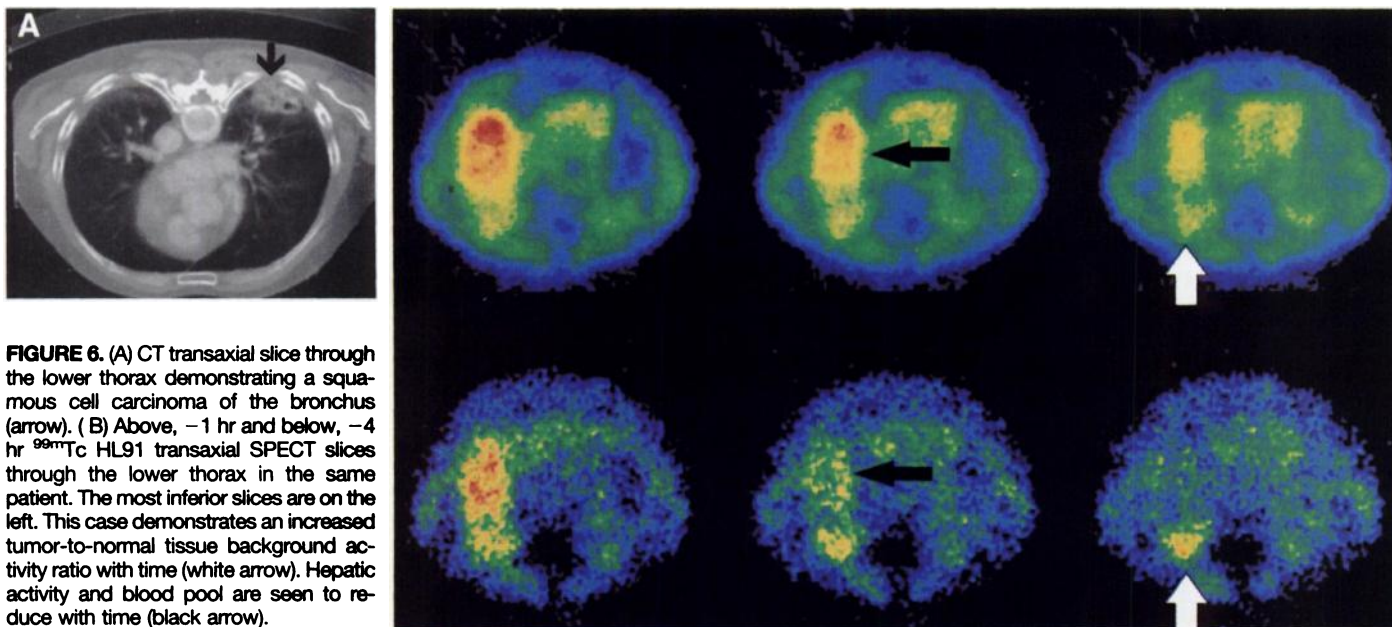


**FIGURE 6.** (A) CT transaxial slice through the lower thorax demonstrating a squamous cell carcinoma of the bronchus (arrow). (B) Above, -1 hr and below, -4 hr  $^{99m}\text{Tc}$  HL91 transaxial SPECT slices through the lower thorax in the same patient. The most inferior slices are on the left. This case demonstrates an increased tumor-to-normal tissue background activity ratio with time (white arrow). Hepatic activity and blood pool are seen to reduce with time (black arrow).

with a single-photon radionuclide, preferably  $^{99m}\text{Tc}$ , would increase availability and allow good quality tomographic imaging.

Several new, hypoxia selective, single photon imaging agents have been described (9,11,13). The chemical basis for these compounds has been to incorporate a 2-nitroimidazole moiety to act as a bioreductive molecule accepting a single electron and producing a free radical anion which, after further reduction, is then incorporated into cell constituents under hypoxic conditions. It has been shown in vitro and in animal studies, however, that the  $^{99m}\text{Tc}$  complexes of the core ligands of some of these compounds show an even greater hypoxia selectivity than compounds with the same ligand donor group with the bioreductive 2-nitroimidazole moiety (11),  $^{99m}\text{Tc}$  HL91 being such a compound.

Several observations in this preliminary study are worthy of note. In six cases, tumor uptake increases with time whereas blood pool is reduced. This suggests a specific tumor uptake mechanism rather than a blood-pool effect in these tumors. However, a comparison is only made in two points in time in a small number of subjects in this preliminary study and further investigation is required to confirm this.

A high proportion of tumors in this study showed accumulation of  $^{99m}\text{Tc}$  HL91. Some of the tumors studied (e.g., squamous cell carcinoma) have a high incidence of hypoxia (3), but hypoxia in other tumors such as lymphoma is less well recognized. Although there is good evidence of hypoxia selectivity in vitro and in animal studies with  $^{99m}\text{Tc}$  HL91 (11), the mechanism of accumulation in human cancers has yet to be clarified. Although  $^{18}\text{F}$ -FDG PET was used to locate sites of tumor activity in this study, it is interesting to note the similarity in patterns of uptake between  $^{18}\text{F}$ -FDG and  $^{99m}\text{Tc}$  HL91, which may suggest a possible shared hypoxic mechanism of accumulation. Although the mechanisms of tumor accumulation of  $^{18}\text{F}$ -FDG are diverse, a correlation with cell hypoxia has been described in human tumor cell lines (15).

T:N ratios are consistently higher with  $^{18}\text{F}$ -FDG-PET than  $^{99m}\text{Tc}$  HL91 in this study. There are several possible reasons for this. Although hypoxia may be a common factor in the accumulation of these radiopharmaceuticals, additional mechanisms are likely to play a part in the uptake of  $^{18}\text{F}$ -FDG. Some

differences may result from the two different imaging methods that have been used, PET and SPECT.

After  $^{99m}\text{Tc}$  HL91 injection, activity was not detected in metastatic sites in two patients in this study. Although high liver activity, due to hepatic clearance of this agent, may have obscured uptake into known carcinoid liver metastases, the lack of accumulation in known supraclavicular lymph nodes in this patient suggests that this tumor did not have a significant hypoxic fraction. This might be expected in a tumor that is characteristically vascular and often is of only a low grade of malignancy (16) and supported by minimal  $^{18}\text{F}$ -FDG accumulation (SUV 0.85) in this case. The apparent lack of uptake into follicular carcinoma of the thyroid metastases may be due to their small size in view of the positive uptake seen in a much larger base of the skull lesion.

## CONCLUSION

In this study, injection of  $^{99m}\text{Tc}$  HL91 resulted in specific localization in the majority of malignant tumors identified by  $^{18}\text{F}$ -FDG PET. Technetium-99m HL91 exhibits good imaging characteristics and imaging at 4 hr provided good lesion-to-normal tissue background ratios that may be further enhanced with SPECT. Additional studies are needed to confirm a hypoxic mechanism of accumulation in humans and to clarify the clinical potential of this agent.

## ACKNOWLEDGMENTS

We thank Amersham International PLC for providing the radiopharmaceutical used in this study.

## REFERENCES

- Gatenby RA, Coia LR, Richter MP, et al. Oxygen tension in human tumours: in vivo mapping using CT-guided probes. *Radiology* 1985;156:211-214.
- Hockel M, Schlenger K, Knoop C, Vaupel P. Oxygenation of carcinomas of the uterine cervix: evaluation by computerized  $\text{O}_2$  measurements. *Cancer Res* 1991;51:6098-6102.
- Gatenby RA, Kessler HB, Rosenblum JS, et al. Oxygen distribution in squamous cell carcinoma metastases and its relationship in outcome of radiation therapy. *Int J Radiat Oncol Biol Phys* 1988;14:831-838.
- Chapman JD. Hypoxic sensitizers: implications for radiation therapy. *N Engl J Med* 1979;301:1429-1432.
- Henk JM, Smith CS. Radiotherapy and hyperbaric oxygen in head and neck cancer. Interim report of second clinical trial. *Lancet* 1977;2:104-105.
- Vaupel P, Schlenger K, Knoop C, Hockel M. Oxygenation of human tumours: evaluation of tissue oxygen distribution in breast cancers by computerized  $\text{O}_2$  tension measurements. *Cancer Res* 1991;51:3316-3322.

7. Chapman JD. Measurement of tumour hypoxia by invasive and non-invasive procedures: a review of recent clinical studies. *Radiotherap Oncol* 1991;20:13-19.
8. Okunieff PG, McFarland E, Rummeny E, et al. Effects of oxygen on the metabolism of murine tumours using in vivo phosphorus-31 NMR. *Am J Clin Oncol* 1987;10:475-482.
9. Nunn A, Linder K, Strauss HW. Nitroimidazoles and imaging hypoxia. *Eur J Nucl Med* 1995;22:265-280.
10. Rasey JS, Kok WJ, Grierson JR, Grunbaum Z, Krohn KA. Radiolabelled fluoromisonidazole as an imaging agent for tumour hypoxia. *Int J Radiat Oncol Biol Phys* 1989;17:985-991.
11. Archer CM, Edwards B, Kelly JD, King AC, Burke JF, Riley ALM. Technetium labelled agents for imaging tissue hypoxia in vivo. In: Nicolini M, Bandoli G, Mazzi U, eds. *Proceedings of the fourth international symposium on technetium in chemistry and nuclear medicine*. 1995:535-539.
12. Shelton ME, Dence CS, Hwang DR, Welch MJ, Bergmann SR. Myocardial kinetics of fluorine 18 misonidazole: a marker of hypoxic myocardium. *J Nucl Med* 1989;30:351-358.
13. Parliament MB, Chapman JD, Urtasun RC, et al. Non-invasive assessment of human tumour hypoxia with <sup>123</sup>I-iodoazomycin arabinoside: preliminary report of a clinical study. *Br J Cancer* 1992;65:90-95.
14. Okada RD, Nguyen KN, Strauss HW, Johnson G. Effects of low flow and hypoxia on myocardial retention of technetium-99m BMS 181321. *Eur J Nucl Med* 1996;23:443-447.
15. Clavo AC, Brown RS, Wahl RL. Fluorodeoxyglucose uptake in human cancer cell lines is increased by hypoxia. *J Nucl Med* 1995;36:1625-1632.
16. Froudarakis M, Fournel P, Burgard G, et al. Bronchial carcinoids. A review of 22 cases. *Oncology* 1996;53:153-158.

(continued from page 9A)

**FIRST IMPRESSIONS**  
**Pain in the Left Thigh**

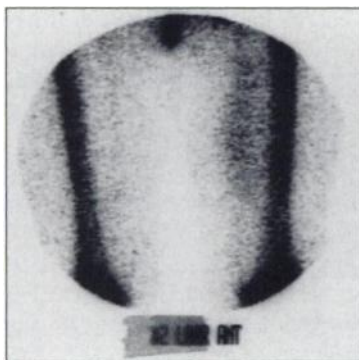


**Figure 1.**

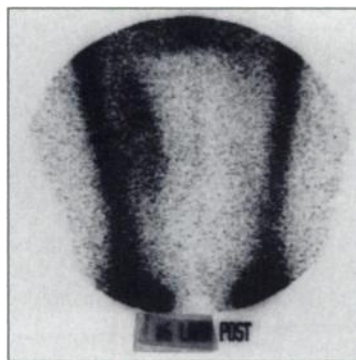


**Figure 2.**

**PURPOSE**

A 48-yr-old woman with symptoms of pain in the left upper leg was referred to nuclear medicine for a bone scan. Radiograph of the area was negative, and there was no obvious clinical evidence of muscle damage. The erythrocyte sedimentation rate was 75 mm/hr. Anterior and posterior views of <sup>99m</sup>Tc-MDP scintigrams of the left and right femoral region demonstrated normal bone scan and marked uptake of radiotracer in the soft tissue corresponding to the left adductor magnum (Figs. 1 and 2). Surgery and histopathology revealed a 16-cm long, highly malignant liposarcoma in the left adductor magnum. Liposarcomas, as well as rhabdomyolysis and muscle injury, are detected by <sup>99m</sup>Tc-MDP.

**TRACER**

Technetium-99m-MDP (400 MBq)

**ROUTE OF ADMINISTRATION**

Intravenous

**TIME AFTER INJECTION**

3 hr

**INSTRUMENTATION**

GE gamma camera

**CONTRIBUTOR**

Bob Dugal, Ostfold Central Hospital Fredrikstad, Norway